THE PENNSYLVANIA STATE UNIVERSITY
SCHREYER HONORS COLLEGE

DEPARTMENT OF BIOMEDICAL ENGINEERING

PEPTIDE COORDINATED IRON OXIDE NANOPARTICLES FOR PRECISION MAGNETIC RESONANCE IMAGING

SAMUEL AJAMU
SPRING 2018

A thesis
submitted in partial fulfillment
of the requirements
for a baccalaureate degree in Biomedical Engineering
with honors in Biomedical Engineering

Reviewed and approved* by the following:

Scott Medina
Assistant Professor of Biomedical Engineering
Thesis Supervisor

Jian Yang
Professor of Biomedical Engineering
Honors Adviser

James Adair
Professor of Material Science
Faculty Reader

* Signatures are on file in the Schreyer Honors College.

ABSTRACT

The current technologies at our disposal for diagnostic imaging consist of CT, X-Rays, Ultrasound, PET, and MRI. Among all of these imaging modalities, MRI is one of the most versatile and detailed instruments for imaging internal organs. It is exceptional because it provides clear differences in abnormal and normal tissues and it does not subject patients to x-rays that could be harmful with repetitive use. This thesis will explore a peptide-based material to enhance the capacity of MRI imaging but specifically to cancer tissue. The material is a peptide- based colloidal material that enables the magnetic resonance imaging of cancer cell. The colloidal material will consist of iron oxide particles and metal- chelating peptide that holds the structure together. This peptide and iron oxide colloid will serve as a contrast agent that are controlled to a specific size to ensure that they utilize a phenomenon in cancer tissue called enhanced permeability and retention effect.

Overall, the purpose of this thesis is to obtain a better understanding of how peptide can be used for imaging materials. The anticipated outcome of this process will be to obtain qualitative and quantitative information on the effectiveness of the uptake of the peptide chelated iron oxide particles. This aimed to verify the production of the iron- oxide contrast agent and the ability to control their size with a high affinity peptide. The data for effective uptake will be taken using Dynamic Light Scattering. This will be done using controls as a way of quantifying the effects of the peptide on the size of the iron oxide particles. Additionally the effectiveness of the nanoparticles will be measured using MRI to view the magnetic effects of the contrast agents. This will be done on just the particles to see if they retain their magnetic properties. The collective data as a whole will show the way a novel contrast agent passively targeting cancer cells can be produced.

TABLE OF CONTENTS

LIST OF FIGURES iii

LIST OF TABLES iv

ACKNOWLEDGEMENTS v

Chapter 1 : Introduction 1

- Peptide Discovery 4
- Peptide Synthesis 5

Chapter 2 : Design 6

Chapter 3 : Results 11

- Synthesis 11
- Particle Characterization 16
- UV-VIS Solubility 22

Chapter 4 : Conclusion 24

BIBLIOGRAPHY 26

LIST OF FIGURES

Figure 1. LC PDA chromatograph of the crude peptide 11

Figure 2. Image of the synthetic peptide TVNFKLYGGGTVNFKLY 12

Figure 3. Mass Spectrometry spectrum of the crude peptide 13

Figure 4. LC PDA Chromatograph of the purified peptide 14

Figure 5. The mass spectrum and m/z plot of the purified peptide 15

Figure 6. Intensity distribution of the nanoparticles without peptide 17

Figure 7. Iron Oxide particles stabilizer solution in water. 18

Figure 8. Intensity vs. size spectrum of NPs in 1 wt. % of triton x-100 in water 19

Figure 9. Volume vs. size plot of a 1 wt. % triton x-100 solution with NPs (with TMAOH stabilizer) 20

Figure 10. Size vs. Peptide Concentration 21

Figure 11. Turbidity at 300nm of varying concentrations of Peptide Particle Solution 22

Figure 12. Plausible Binding Theory of Peptide to Particles. 23

LIST OF TABLES

Table 1. Peptides with high binding affinity for Magnetite Nanoparticles. 5

Table 2. Reagents used in a 0.1 scale synthesis of TVNFKLYGGTVNFKLY 7

Table 3. The amino acids in the sequence and the coupling method used for optimal synthesis 8

Table 4. Coupling of the 0.25mM synthesis 9

Table 5. Reagents used in a 0.25mM scale synthesis of TVNFKLYGGTVNFKLY 10

Table 6. Cleavage cocktail 1 10

Table 7. Reagents and ratios for TIPS cleavage 11

Table 8. The charged state and m/z value of TVNFKLYGGGTVNFKLY 12

ACKNOWLEDGEMENTS

Special thanks goes to the Precision Therapeutics and Bioresponsive Materials Lab and specifically to Dr. Scott Medina. His assistance and advice were invaluable to the completion of this thesis. Additionally, Dr. Hayes' Lab especially Jonathan Casey was helpful and willing to provide his help in particle acquirement and troubleshooting. Thanks also reserved for Dr. James Adair as his input and contribution made the MRI section possible.

Chapter 1 : Introduction

The focus of this thesis is to develop a contrast agent to first improve MRI contrast buts also is preferentially delivered to tumor tissue. In order to do so, understanding what an MRI does is a crucial aspect in determining the method in which to pursue constructing a contrast agent. Magnetic resonance imaging is described as, using the body's natural magnetic properties to produce detailed images from any part of the body. For imaging purposes, the hydrogen nucleus or proton is used because it is ubiquitous in the human body. The protons are best compared to magnets, each having its own north and south pole.[1] Under normal circumstances, the protons spin in the body with their axes randomly aligned. When the body is placed in a strong magnetic field, as that of a MRI scanner, the protons' axes all line up. This uniform alignment creates a magnetic vector oriented along the axis of the MRI scanner.[1] The protons are then subjected to pulsing radiofrequency that disrupts the protons' alignments with magnetic vector. The realignment of the protons then releases energy release. This energy is sensed and used to produces an image of the tissue sample. There are material that have been identified to have the ability to make this signal stronger or weaker which can produces imaging contrast at the material site. These materials work by propagating the magnetic field on the molecular level and are the agents used to produce enhanced contrast in an MRI. The strength of the magnetic field can be altered from head to toe using a series of gradient electric coils. In doing so, the local magnetic field is altered by these small increments and different slices of the body will resonate as different frequencies are applied."[1] This means that specific parts of the body can be focused on and different depths can be achieved with the use of an MRI. Therefore, the material located at different regions of the body will create localized enhancement in image contrast for MRI.

The time taken for the protons to fully relax is measured in two ways. One time looks at the duration of the the magnetic vector to return to its resting state back into alignment with the external magnetic field and the other is time the axial spinning of each proton returns to its resting state. The first is called T1 relaxation, and the axial spinning relaxation is the T2 relaxation. Predominately, T1 relaxation contrast agents produce brighter images and T2 relaxation contrasts produce darker images.

In proceeding with exploring MRI options of this thesis, another attribute of this method of imaging that sets it apart from other imaging modalities is that there are no known biological hazards of MRI. Unlike x-ray and computed tomography, MRI uses radiation in the radiofrequency range. This frequency has been known to not produce harmful exposure to tissue. This makes MRI an innovative technique that provides images of the body in many different planes and depth without the fear of harmful exposure. Its images also vary based on the chemical and molecular environment of this tissue. This makes it a powerful diagnostic tool for the fight against many diseases.

Therefore, with the MRI instrument being robust and capable of these images, enhancing the capabilities of this instrument will go a long way in faster diagnostic times. On the subject of cancer specifically, MRI stands as power diagnostic tool because the treatment times are a crucial component in determining the curability of this disease. Currently there are contrast agents that are being used to propagate the magnetic signal produced by the MRI machine. These agents include metals such as gadolinium. This agent is known to be a T1 relaxation contrast and is common due to its high contrast capabilities. This shortened time is directly related to the signal strength that will be observed in the image. However even though gadolinium based contrast agents have been used the toxicity of these agent to the human body are still under debate. As a heavy metal, gadolinium is extremely toxic in its free form. These agents also have the tendency to accumulate in patient's bones and brain. Another agent that has been known for its contrast abilities but lack of clinical application is iron oxide (IO) nanoparticles.

Unlike gadolinium-based agent, these particles cannot produce the same quality of contrast. It however does not pose the same toxicity risk as does the gadolinium-based agents.

While exploring the idea of (IO) particles further due to their non-toxic nature, the task of improving their contrast capabilities must be addressed. One potential option of increasing contrast capabilities is by simply increasing local concentrations of IO particles at the imaging site. With this idea being viable because IO particles have such low toxicity to the body, active and passive targeting schemes can be designed for them. When addressing specifically cancer cells, there are different methods of using active and passive targeting. Active targeting could be achieve by merely conjugating target ligands on to the surface of the IO particles. These target ligands will have a high affinity of the tumor tissue receptors. Passively targeting tumor tissue is a systemic approach. The main course of doing so would utilize a phenomenon called the enhance permeability and retention affect.

The idea behind the enhance permeability and retention affect is there are unique structural defect that can be taken advantage of by particles. In fast growing cancer cell, the endothelial surface is fenestrated with gaps between endothelial cells, and is surrounded by discontinuous or absent basement membranes. The defective endothelial barrier function is one of the best-documented abnormalities of tumor vessels.[11] Blood vessel leakiness enables macromolecules to reach tumor cells from the bloodstream. It allows these molecules to deposit in this interstitial space and because of the weak lymphatic systems of cancer cell, the deposited molecules or particles are not cleared. However, in order for these molecules to passively enter this region they have to be of a certain size distribution. The idea is to use IO or magnetite particle, known for its MRI capabilities and control its size so that it can take advantage of this phenomenon. The contrast agent will then preferentially target tumor tissue. This increased localization will then produce enhance contrast when imaged using a MRI.

In an attempt to understand how IO particles are produce and were used previous formulation of IO particles were examined. The IO contrast agent formulations such as resovist, used in the past-

included solutions that could coat the IO particles. These particles are in need of coating because they tend to aggregate in an aqueous solution. Hydrophobic interaction take affect and they agglomerate to each other. From this fact, these particles do not produce a stable solution and could not be viable for intravenous use. Due to the characteristic of these particles, coating have to be used in order for them to remain stable for clinical use. Carbohydrates such as dextran were common for IO formulations and needed to provide the stability necessary for intravenous use. However, these formulations became obsolete due to the toxicity of dextran to patients.

So with the necessary presence of coatings on IO particles, biological based coating such as carbohydrates can be considered. The idea behind controlling the size of these particles is also necessary if the particles are to utilize the EPR effect. Therefore, this material must be capable of coating and coordinate the IO particles. The biological coating option that could potentially perform both tasks is a peptide. With a peptide, a high affinity coating can be optimized for the IO particles. Additionally options for adding a bioactive ligand to actively target specific regions is viable with a peptide coating. It can act in these roles while still making the particles more disperse in an aqueous solution. So overall, the idea of exploring a peptide biological coating over a non- biological one provides more design options. Therefore, the focus turns to finding a peptide that can perform these tasks.

Peptide Discovery

Upon consulting literature to assess peptide sequences tested for their binding affinity for magnetite, one that screened sequences using phage display was found. The idea behind the experiment was that a phage library was made using bacteriophages to construct small 7-mer amino acids. These were then inclubated with magnetite nanoparticles and screened for binding affinity. The binding affinity was determined post incubation and after washing the sample of phages and particles mixture. The phages that were retained or that were bound to the magnetite particles were analyzed for the peptide sequence

they displayed. The peptides were 7 amino acids long and the ones that had the highest binding affinity to magnetite (Fe3O4) were found to be those in the table below. The bonding affinity was quantified by the phage clones recovered.

Sequence	#AA	Binding Affinity (Recovery of Phage Clone)
TVNFKLY	**7**	**4.5E-4**
HYIDFRW	**7**	**2.3E-4**

Table 1. Peptides with high binding affinity for Magnetite Nanoparticles.

The sequence with the higher binding affinity or recovered phage clone was chosen for the task of coating and coordinating the particles purely because it had the higher affinity and did not contain histidine residue, which are difficult to synthesis. The peptide chosen was TVNFKLY.

Peptide Synthesis

The most common way of synthesizing peptides is using solid phase peptides synthesis. CEM has developed a patented process for applying microwave irradiation to both the deprotection and coupling steps for an overall more efficient solid phase peptide synthesis. This is the synthesis instrument used to create the peptides. Even though the instrument is optimized for generic peptide synthesis, for specific peptides the method of synthesizing are optimized externally before the instrument engages in it coupling cycles.

The SPPS is a process where peptides residues are chemically bonded in a step-wise fashion while being anchored to an insoluble support called a resin. The carboxyl end of every new amino acid is activated and is coupled with the α-amino group of the previous amino acid. The α-amino group of the

new residue is protected as to not cause unwanted reaction at those sites. The α-amino of that new residue then becomes de-protected after the next residue is ready to be coupled on the sequence. Likewise, because many amino acids have side chains with functional groups that have the ability to react and polymerize other amino acids at those ends, they are also protected throughout the entire synthesis reaction. The sequence then grows with each sub-sequential protecting and de-protecting step until the entire sequence is complete. Also thermodynamically more reagents are added in order to drive each reaction forward and produce the greatest possible yield of the sequence. This comes into play with sequences that are difficult to synthesize and for those that are larger in length. In the case of difficult peptide synthesis, other avenues are explored to ensure the sequence is synthesized successfully. Variables like the swelling of the resin and the loading capacity of the resin can be altered. Additionally the amount of coupling reactions of each specific amino acid residue can be amended to increase the probability that an amino acid will be coupled on to the desired site. Other components that come into play when considering the successful synthesis of a peptide includes the cleavage reactions that are done post synthesis to remove the protecting groups that are place on the side chains to prevent unwanted side couplings. These cleavage reactions can also be optimized to increase the success of the synthesis by eliminating the protections groups.

Chapter 2 : Design

The peptide has a bidentate design with two binding sites for iron oxide nanoparticles. The sequence is TVNFKLYGGGTVNFKLY. The two magnetite-binding sites have the sequence TVNFKLY. These sites are separated by three glycine amino acids. This is to space out the iron oxide nanoparticles from each other. In synthesizing the peptide, many iterations were performed to optimize the synthesis. The charts shown below are different syntheses.

Peptide Synthesis:

0.1mM scaled Synthesis

CEM amino acids obtained at 0.2M concentration

Reagent	Volume (ml)	Mass(g)
Asparagine	11	1.32
Glycine	16	0.96
Leucine	11	0.78
Lysine	11	1.04
Phenylalanine	11	0.86
Threonine	11	0.88
Tyrosine	11	1.02
Valine	11	0.75
DMF	236	-
Piperazine	11.4 w/45.6 DMF	-
DIC	4.18 w/ 49.82 DMF	-
Oxyma	36	5.12
Resine (low loading)	-	0.5

Table 2. Reagents used in a 0.1 scale synthesis of TVNFKLYGGTVNFKLY

The amino acids were all weight out using a calibrated balance and placed into a conical tube. The volume of dimethylformamide (DMF) associated with each amino acid was place in the tube and vortex until the mass was completely soluble. Upon completion, the Liberty Blue Automated Microwave Peptide Synthesizer was calibrated.

In order to the calibration, conical tubes were filled with 10 mL DMF and placed in the locations of the amino acid reagents. Then on the liberty blue software, a maintenance process was run by having

the instrument draw up 5 mL of DMF from each of the reagent positions and dispensing it into the reaction vessel. This amount was then corroborated with the fluid height on the reaction vessel to ensure that the volume dispensed was correct.

Following the calibration, the reaction vessel was cleaned and the filter frit of the vessel was washed and sonicated with methanol for 5 minutes. Then the resin was poured into the assembled reaction vessel and the tubes connecting the reaction vessel to the instrument secured and tighten. The method of the liberty blue software was set to have all the amino acids double coupled in the sequence.

Reagent	**Coupling**
Asparagine	Double coupled
Glycine	Double coupled
Leucine	Double coupled
Lysine	Double coupled
Phenylalanine	Double coupled
Threonine	Double coupled
Tyrosine	Double coupled
Valine	Double coupled

Table 3. The amino acids in the sequence and the coupling method used for optimal synthesis

The instrument was then ran to with the reagents loaded and the resin placed in the reaction vessel. Upon completion of the synthesis, the thermometer that was placed in the reaction vessel to monitor temperature was rinsed with ethanol to ensure that the largest amount of product is recovered. This resin was then taken from the reaction vessel and rinsed with DMF and dichloromethane (DCM). This was done under a vacuum. The sample was allowed to dry for 5 minutes and then placed on a lyophilized overnight to remove residual moisture.

0.25mM scaled Synthesis

Reagent	Coupling
Asparagine	Double coupled
Glycine	Double coupled
Leucine	Double coupled
Lysine	Double coupled
Phenylalanine	Double coupled
Threonine	Double coupled
Tyrosine	Double coupled
Valine	Double coupled
TVNFLKYGGTVNFKLY	The red amino acids were single coupled instead of double coupled for aggregative reasons.

Table 4. Coupling of the 0.25mM synthesis

CEM amino acids were obtained at 0.2M concentration

Reagent	Volume (ml)	Mass(g)
Asparagine	11	1.32
Glycine	16	0.96
Leucine	11	0.78
Lysine	11	1.04
Phenylalanine	11	0.86
Threonine	11	0.88
Tyrosine	11	1.02
Valine	11	0.75
DMF	259.45	-

Piperazine	11.4 w/45.6 DMF	-
DIC	4.18 w/ 49.82 DMF	-
Oxyma	36	5.12
Resine (High loading)	-	0.41

Table 5. Reagents used in a 0.25mM scale synthesis of TVNFKLYGGTVNFKLY

The procedure used for 0.25mM synthesis is identical to the 0.1mM synthesis

Peptide Cleavage

The lyophilized resin was placed into a 20ml scintillating vial, with reagents in the ratio below.

Reagent	**Percentage.**	**For a 10 mL solution**
TFA	90%	9 mL
Thioanisole	5%	0.5mL
Ethanedithiol	3%	0.3mL
Anisole	2%	0.2 mL

Table 6. Cleavage cocktail 1

The reaction mixture was purged with argon and stirred for 3 hours. After this, the reaction was filtered through a fritted funnel. The filter was rinsed with TFA to ensure maximum product retrieval. Then the collected peptide solution was dried over argon until it formed into thicker consistency. This was then precipitated with cold ether and centrifuged down twice. The other method of cleavage uses the same steps but the amended aspect was the cleavage cocktail. The reagents and percentages of the cocktails are shown in table below.

Reagent	**Percentage.**	**For a 10 mL solution**
TFA	95%	9.5 mL
Water	2.5%	0.25mL

TIPS	2.5%	0.25mL

Table 7. Reagents and ratios for TIPS cleavage

Chapter 3 : Results

Synthesis

The peptide sequence of TVNFKLYGGGTVNFKLY was synthesized using microwave synthesis. The purity of the sample is obtained by analyzing the crude peptide. This was done via high pressure liquid chromatography with methylated silica gel stationary phase. The mobile phase increases by 1%/min of B solution (90% acetonitrile, 9.9% water, 0.1% formic acid). At a specific concentration of B solution the peptide will push out the peptide. The resulting chromatograph is displayed below.

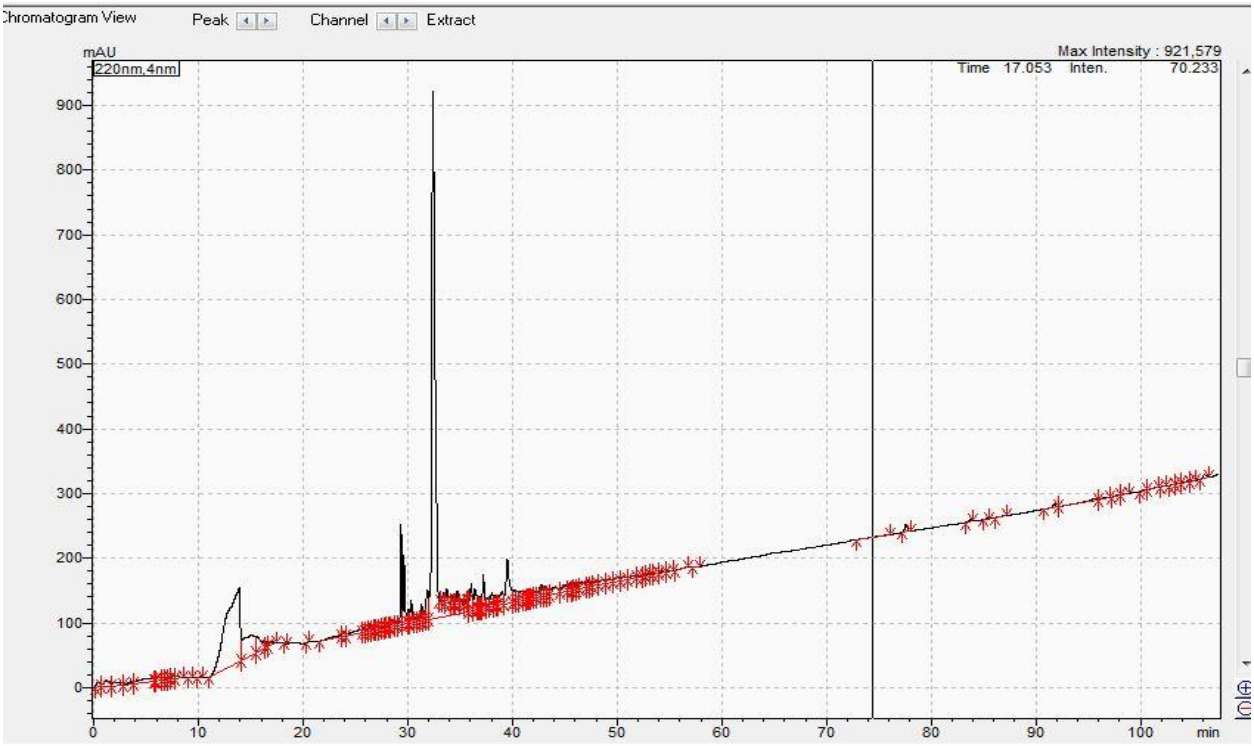


Figure 1. LC PDA chromatograph of the crude peptide

The chromatograph shows a major peak at around 32 minutes. This peak is significant in terms respects to the other peaks because of its magnitude. This fact could denote that the synthesis was successful if this major peak belongs to the peptide. The other data that needs to complement this in order to verify the successful synthesis of the peptide is the mass spectrometry data. This data gives the mass over charge ratio which can be indicative of the desired peptide. The desired peptide is shown below and has the m/z values. It has three potential charged states so has there

indicative m/z values.

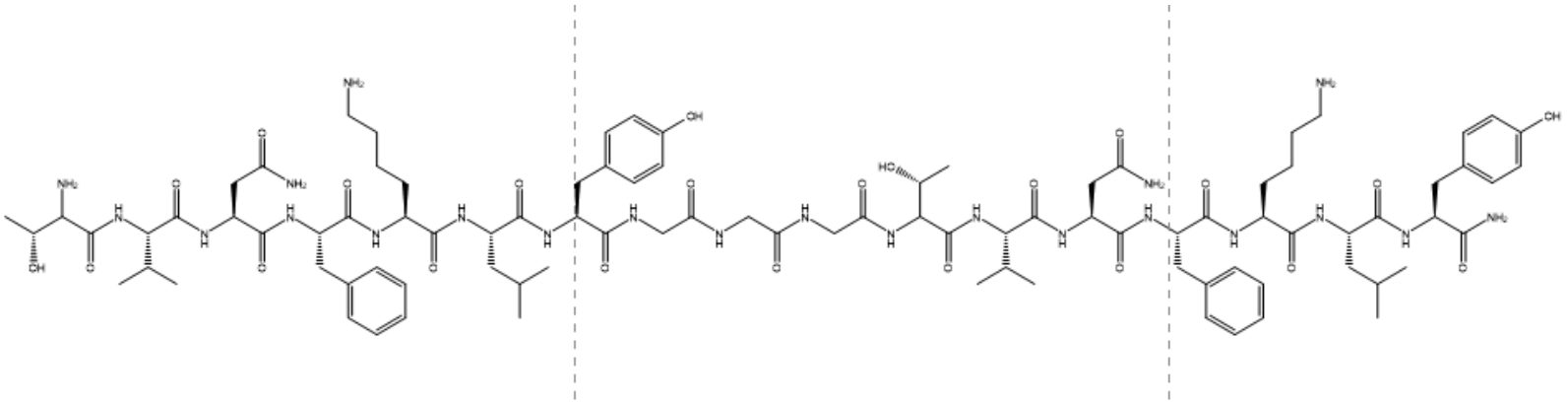


Figure 2. Image of the synthetic peptide TVNFKLYGGGTVNFKLY

The charged state and m/z values are shown below. The three potential charged states are located on the terminal threonine and the side chains of the two lysine residues in the sequence.

Charged State	**m/z**
M + 1	1920.03
M + 2	960.52
M + 3	641.02

Table 8. The charged state and m/z value of TVNFKLYGGGTVNFKLY

Upon running the sample through the mass spectrometry, the following spectrum below was produced. Recalling on the time the major peak appeared on the liquid chromatography spectrum, the data can be correlated with that of the mass spectrometry to see what the m/z value for that peak. The time was 32 minutes and this correlates with another major peak on the MS spectrum. This peak like the PDA chromatograph is higher in intensity than all the other peaks adjacent to it. The peak has an m + 1H peak of 1921.1. It has an m + 2H peak of 960.8. And lastly it has an m + 3H peak of 641.2. These are all ion peaks that denote that there was a successful synthesis of the iron oxide high affinity peptide.

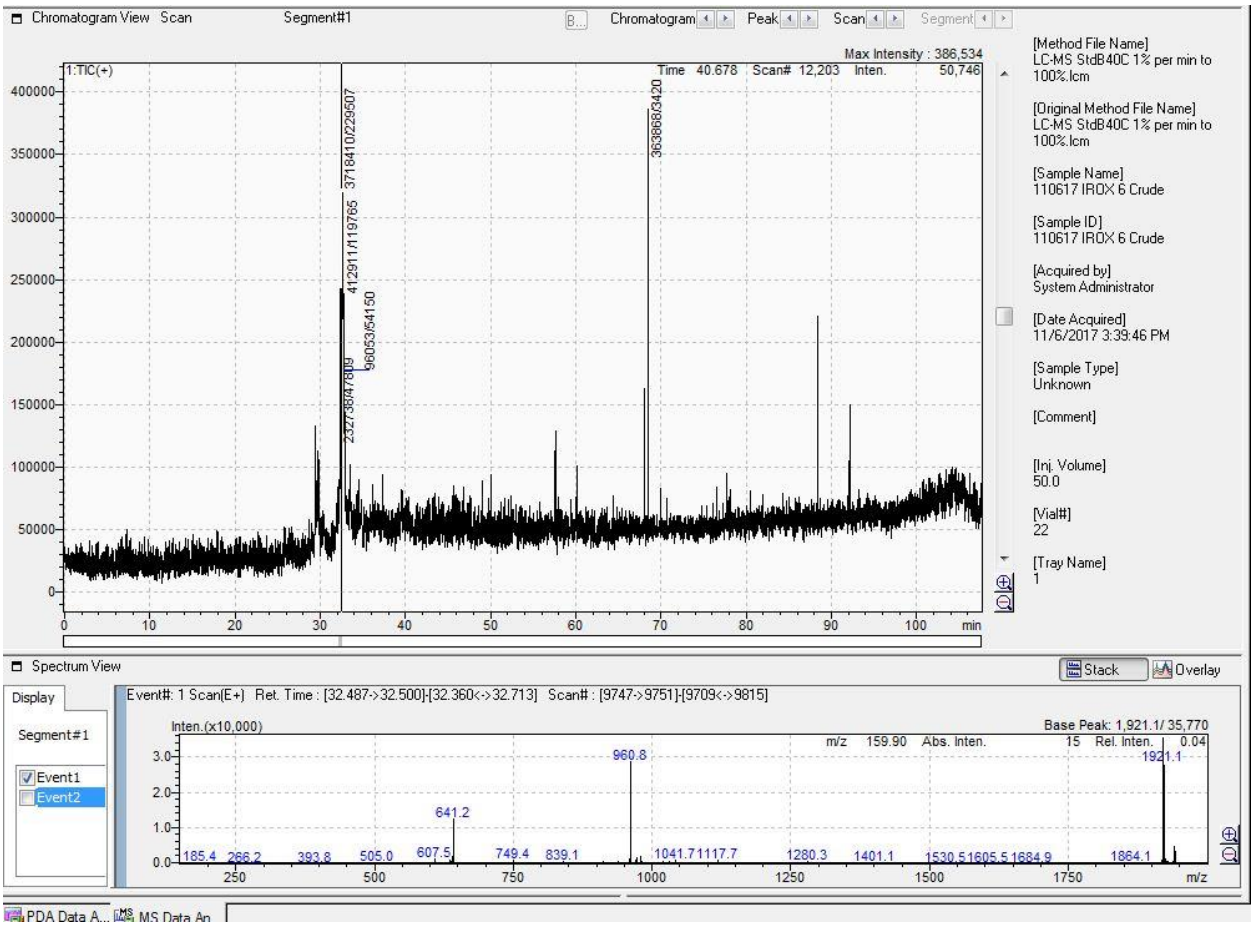


Figure 3. Mass Spectrometry spectrum of the crude peptide

Additionally when observing the mass spectrum, it is clear that an impurity peak is present before the desired peak, however this peak tappers off completely before the desired starts to rise. This is a beneficial feature of the sample because this means that upon purification, impurities are less likely to be collected with the peptide peak. Additionally, the ion spectrum of the peptide peaks shows no impurity close in intensity to the three m/z values of the peptide. This means that within the peptide peak there are no significant impurities that will be present. For the most part the value peak is purely the desired peptide. This relatively successful synthesis was obtained after the synthesized peptide was cleaved in a TIPs cocktail described further in the methods. Due to the successful synthesis, the sample was purified via a preparative high pressure liquid chromatography. After collection of the purified sample, the sample was run using liquid chromatography and mass spectrometry to verify that the peak was collected. The PDA data for the purified sample is shown below.

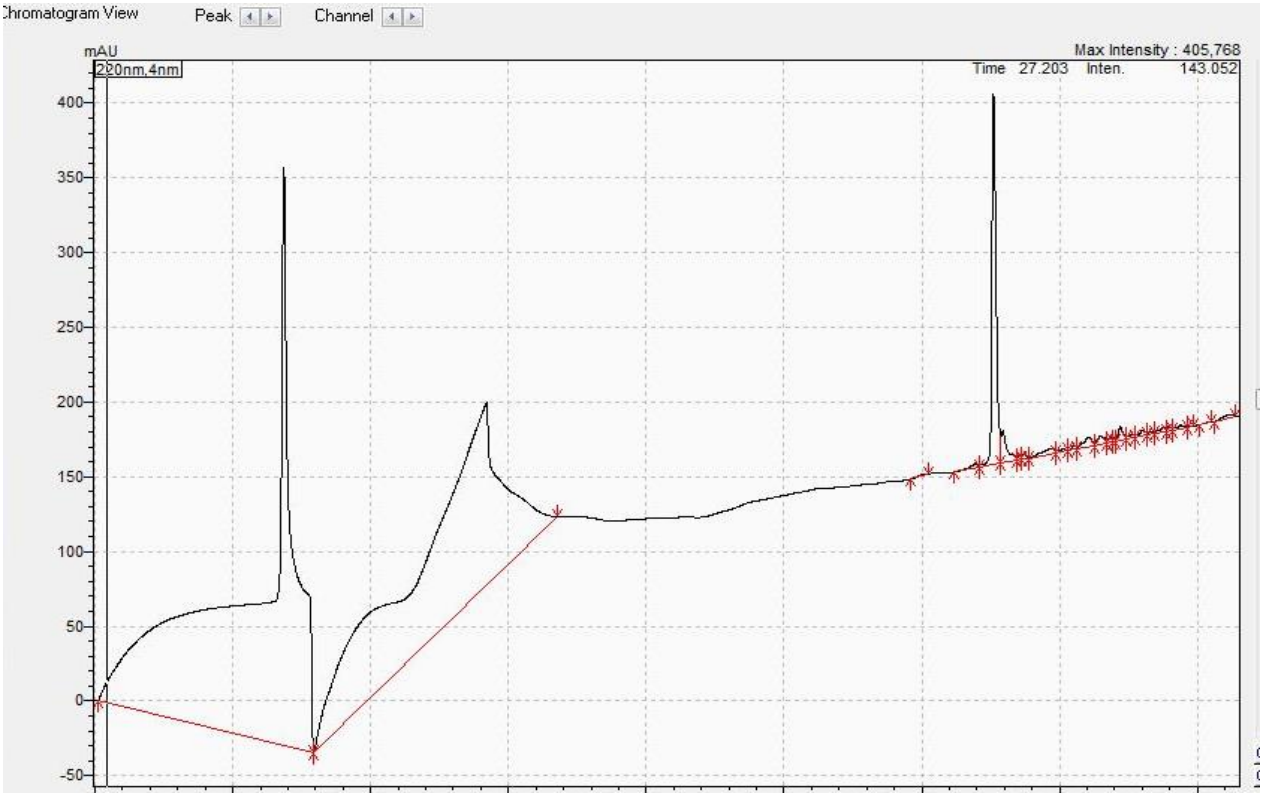


Figure 4. LC PDA Chromatograph of the purified peptide

Due to the clean singular peak of the chromatograph post solvent front, shows a single pure sample was obtained. The peak is singular unlike that of the crude sample. This shows that with a there are no little to no impurities present in the sample. If the sample contains the desired peptide's m/z values then the purification process would be deemed successful as well. Additionally from the chromatograph, we can observe that the profile of the peak is narrow. This means that the collected sample is quite uniform than if the peak was observed to be broad and wide. Now when examining the mass spectrum, there is a clear peak at around 32 minutes. This elution time is also identical to the major peak observed in the crude spectrum, which gives additional evidence that this peak belongs to the successfully synthesized peptide. In examining the mass spectrum of the purified peak, we can solidify the purity of the sample. The spectrum is shown below.

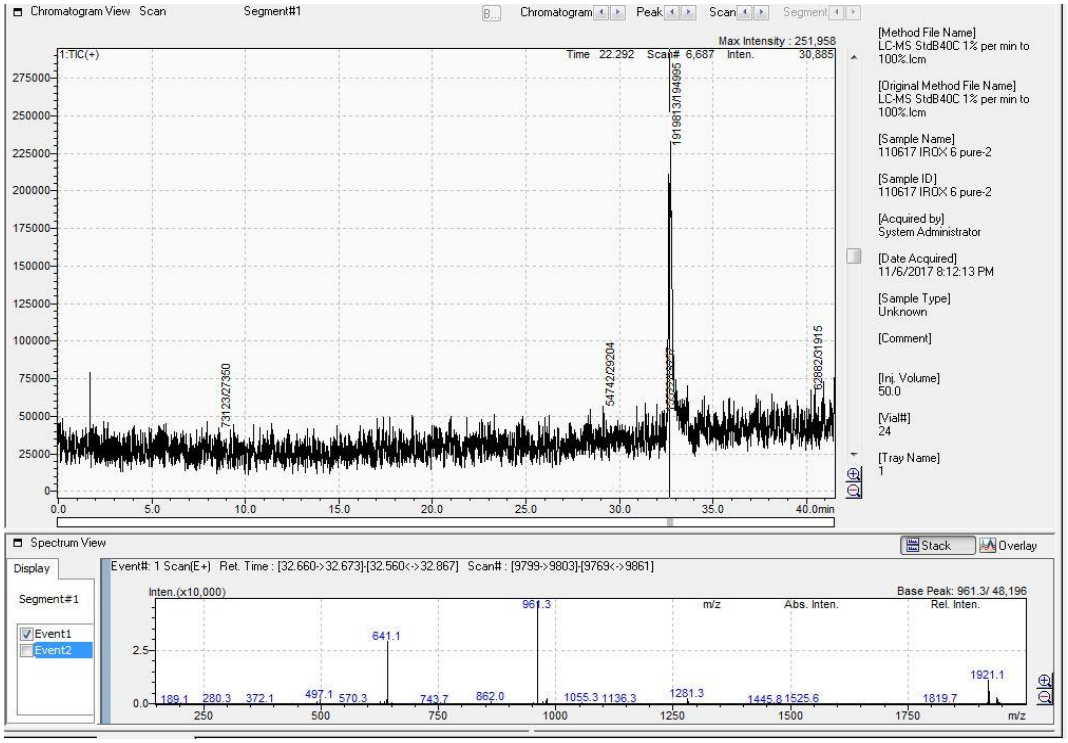


Figure 5. The mass spectrum and m/z plot of the purified peptide

The spectrum shows a single peak similar to the PDA chromatography. The peak does not have a shoulder or other impurities near it which means that the sample is purely one substance. When deciphering the m/z plot for this singular peak, it contains the m/z values shown in table X that belong to the desired peptide. The ions are quite high intensity compared to the values of the highest impurities. This means that the sample is quite pure because the impurity peaks are insignificant when in the peptide peak. Additionally, the peaks is quite narrow and sharp which indicates that the peptide was not

Particle Characterization

Upon successful synthesis and purification of the peptide, experiments with the iron oxide particles and the peptide were performed. The first experiment focused on answer one question. The question is whether the peptide has the ability to coordinate iron oxides particles to form a colloid. The colloid consists of the peptide evenly distributed within the solid of iron oxide nanoparticles. This was done using an aqueous solution of iron oxide particles in tetra-methyl ammonium hydroxide. This allowed the particles to be more soluble in a peptide rich aqueous solution. Upon incubating the nanoparticles in the different concentrations of peptide, the samples were measured using DLS. The figure below shows the results of the negative control. This was the nanoparticle solution without incubating in peptide. The aqueous solution consist of pure water. The solution was diluted 1:100 to ensure that it was suitable for DLS measurements. The solution contained 10uL of particles in stabilizer and 990uL of water.

		Size (d.nm):	% Intensity:	St Dev (d.nm):
Z-Average (d.nm): 132.4	Peak 1:	133.4	100.0	49.46
PdI: 0.321	Peak 2:	0.000	0.0	0.000
Intercept: 0.939	Peak 3:	0.000	0.0	0.000
Result quality : Good				

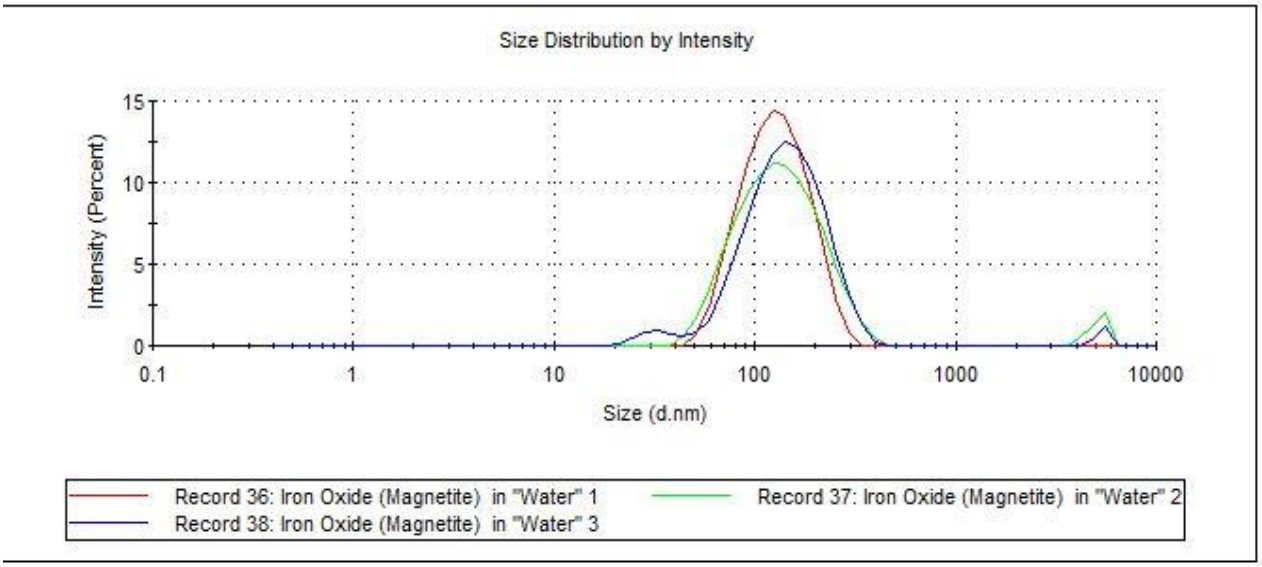


Figure 6. Intensity distribution of the nanoparticles without peptide

The figure shows the purely synthesized particles in an aqueous solution. The DLS intensity spectrum shows that the particle are centered around 100 nm. This means that without the peptide the particle are already at a value which fits into the enhance permeability and retention range. This spectrum is a plot of intensity and size, which means that the particles with in the 100 nm range scatter the most amount of light. When examining the same sample with volume percentage vs. size. This spectrum is shown below.

		Size (d.nm):	% Volume:	St Dev (d.nm):
Z-Average (d.nm): 132.4	Peak 1:	123.9	100.0	61.63
Pdl: 0.321	Peak 2:	0.000	0.0	0.000
Intercept: 0.939	Peak 3:	0.000	0.0	0.000

Result quality : Good

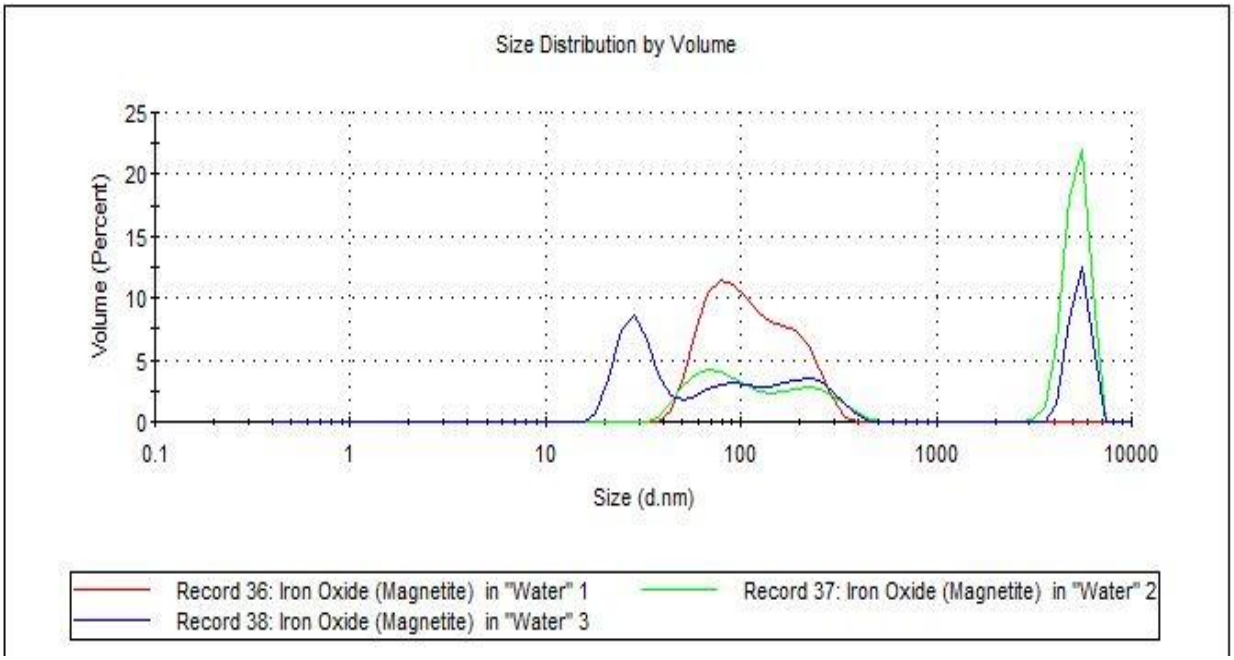


Figure 7. Iron Oxide particles stabilizer solution in water.

This volume vs. size plot shows that the volume of particles in the solution are wide spread amongst the sizes. There is a significant amount of volume in the 100 nm region as well as in the region approaching the 10,000 nm. This means that particles are not uniformly dispersed but contain a diverse range. In order to ensure to meet the goal of using peptides to construct colloids that fit into the 50-100 nm range, the particles have to become more monodispersed. In order to do so other surfactants or methods have to be explored. One method that was explored was the use of Triton x-100 to make the particles more monomeric. The

method uses a 1 wt. % of triton x-100 in water to dilute the particles. The attempt at producing more monomeric iron oxide particles produced the following DLS spectrum.

			Size (d.nm):	% Intensity:	St Dev (d.nm):
Z-Average (d.nm):	32.45	Peak 1:	134.4	71.4	80.62
PdI:	0.957	Peak 2:	9.632	25.7	2.631
Intercept:	0.931	Peak 3:	4303	2.9	966.6
Result quality :	Refer to quality report				

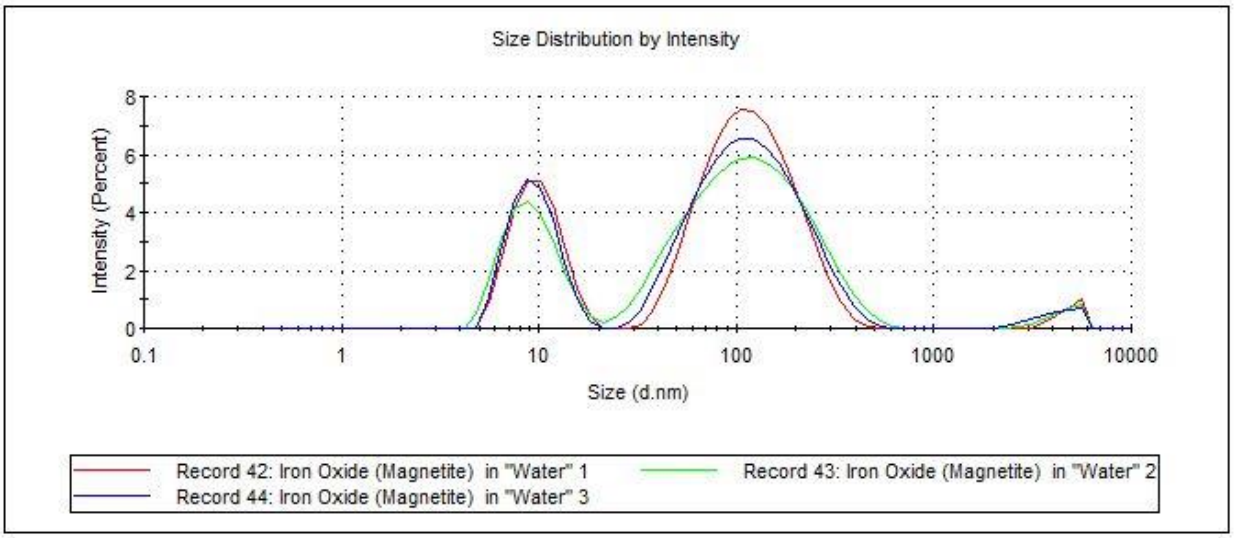


Figure 8. Intensity vs. size spectrum of NPs in 1 wt. % of triton x-100 in water

This data shows that there are now particles centered on the 10 nm range. However, a large amount of intensity is still centered on a 100 nm region. The volume spectra will be beneficial to observe the true distribution of the sample. The following figure shows the volume vs. size of the sample.

		Size (d.nm):	% Volume:	St Dev (d.nm):
Z-Average (d.nm): 33.34	Peak 1:	8.178	99.2	2.273
PdI: 0.970	Peak 2:	73.54	0.4	33.55
Intercept: 0.935	Peak 3:	246.2	0.1	70.30

Result quality : Refer to quality report

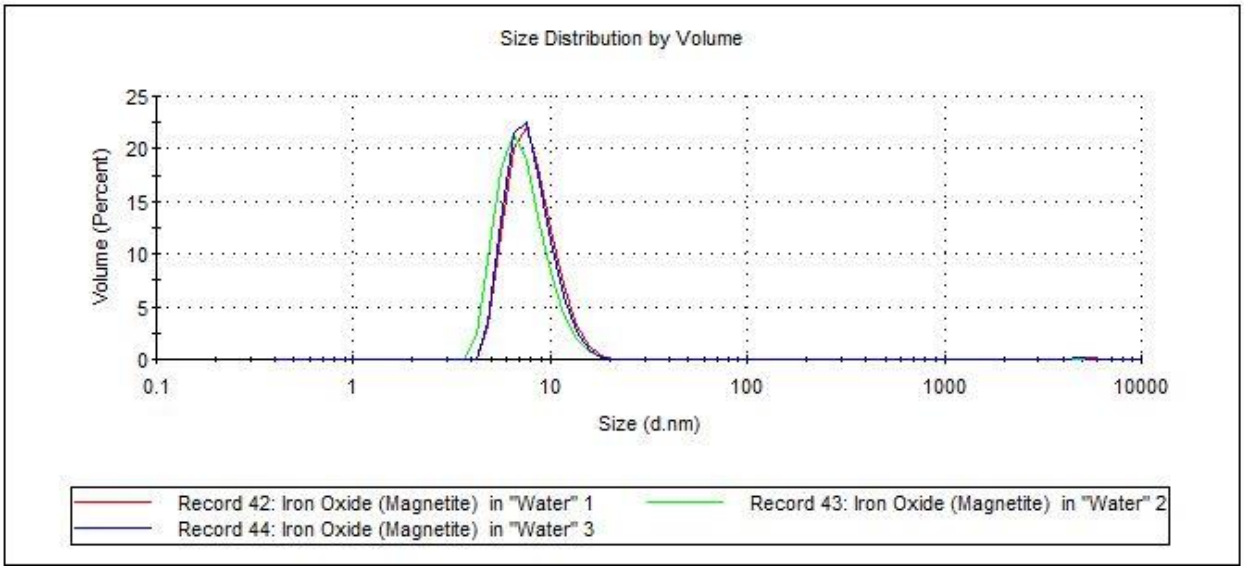


Figure 9. Volume vs. size plot of a 1 wt. % triton x-100 solution with NPs (with TMAOH stabilizer)

This plot shows that the majority of the volume of particles in the sample are within the 10nm region. However, on further evaluation of the sample and the buffer solution (1 wt. % triton x-100 solution in water) shows that the buffer which contains no particles also contains a signal in the 10 nm region. This means that particles are not responsible for the signal in the 10 nm region. An alternative explanation of the signal in the 10 nm region could be the fact that triton x-100 is an amphiphilic molecule which means it is more prone to forming micelles. These could potential be the root of the signal in the 10 nm region.

The next stage of the DLS experiments neglected the efforts to produce more monomeric states of magnetite particles. This process looked into exhibiting size control of these particles in an aqueous medium. Magnetite in tetramethylammonium hydroxide was taken at a volume of 0.5

mL and washed with methanol and dried over argon. These nanoparticles were then incubated with the 1mL of iron oxide binding peptide at different concentrations. After an hour of incubation at physiological temperature, the particles were allowed to settle. Large insoluble aggregates were allowed to crash our in solution. The supernatant of these particles were then taken and diluted 1:100 in water and taken for DLS measurements. The results of two replicates of this experiment is shown below.

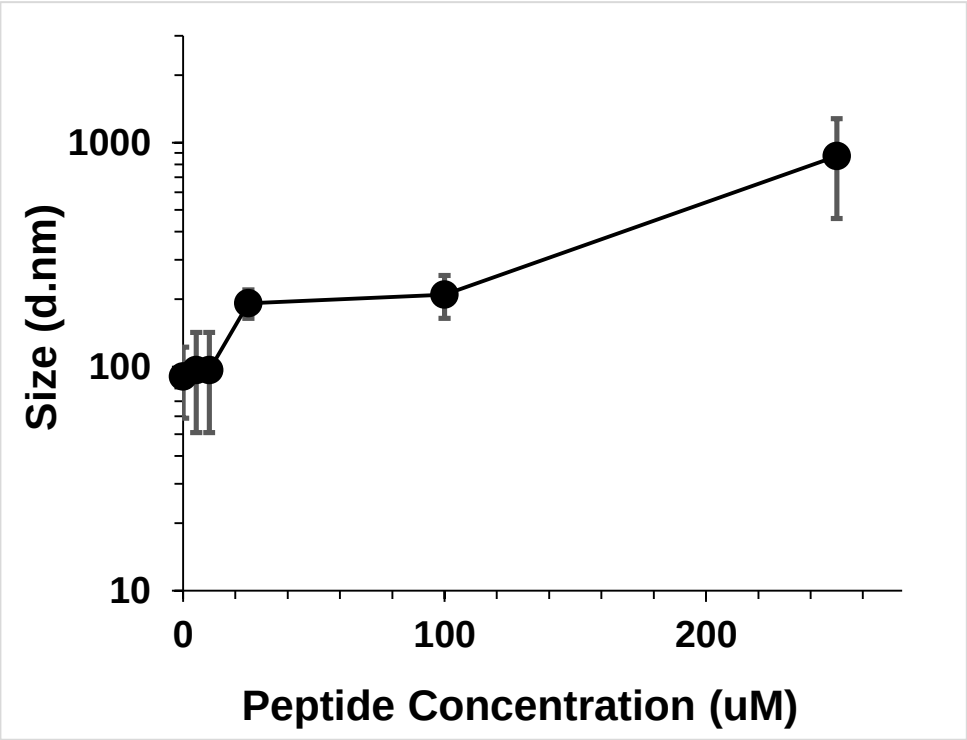


Figure 10. Size vs. Peptide Concentration

This plot shows that the particles are not single sized to begin with. This is because the particles start at a hydrodynamic diameter of 100nm. This means that the particles are aggregate like expected because the size distribution should be about 20nm. Additionally this plot shows two specific three size regions. One where the particles have not changed with increase in peptide concentration, another where the particles are at about 200nms and the last where the particles jump to a size of 1000nm.

In order to further understand the binding behavior and size growth of these particles other experiments were done.

UV-VIS Solubility

Concurrent with the preparation of the DLS samples, UV-VIS samples were also created. From the incubated vial 5uL of the peptide/iron oxide mixture were taken and diluted 1:100 in water. The turbidity of the particles at varying concentration of peptide was obtain. The idea is that this provides the fractional solubility of magnetite nanoparticles at a specific concentration of peptide. A wavelength was selected to compare the absorbance of the samples uniformly. The trend of the plot is shown below.

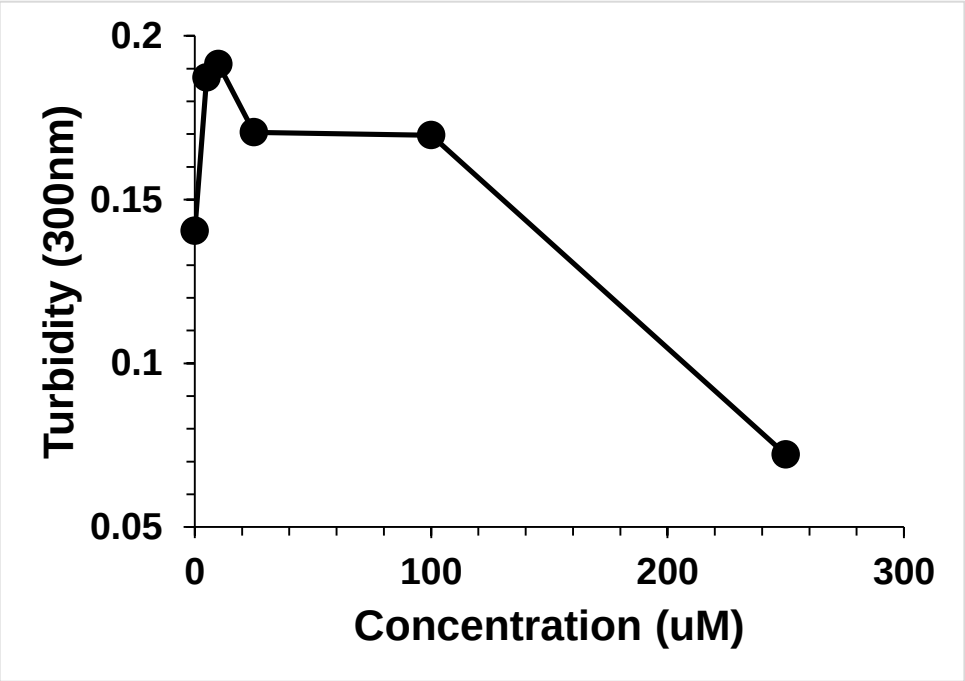


Figure 11. Turbidity at 300nm of varying concentrations of Peptide Particle Solution

While examining this data, it shows that at low concentrations of peptide there is an increase in turbidity of the particles. This means the particles are more dispersed in solution because naturally the

particles absorb light and more disperse particles will do this much better than non-dispersed ones. There is then a drop off in turbidity that stays constant until 100uM of peptide concentration and then a significant drop at 250uM. In order to better understand these sets of data, the plots were contemplated and compared to see if any trends exist between them. The figure that shows the process is shown below.

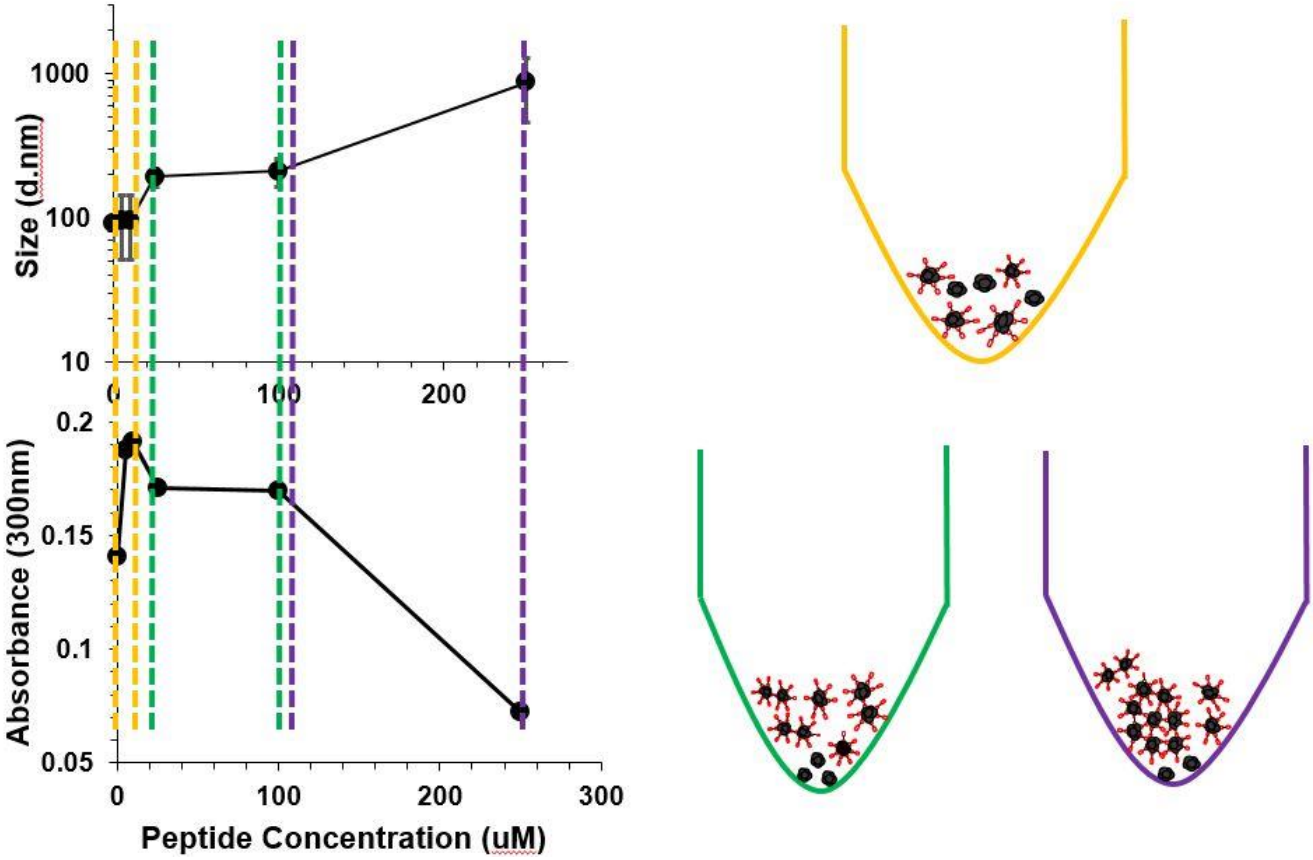


Figure 12. Plausible Binding Theory of Peptide to Particles.

The explanation that is most plausible for these two data sets is a three-stage story. The first stage looks at the region with no size growth but high absorbance/ turbidity. This is indicated with the yellow dashed lines on both plots. The theory that explains this condition is that the particles are increasing in dispersion because the peptide is coating the particles. However, there is no size growth because not enough peptide is present to coordinate the nanocluster to increase the overall size. An image depicting this is shown in the yellow test tube. The second stage is the region with medium size and medium

absorbance or turbidity. This region shows that the nanoclusters are beginning to coordinate into a larger size because of the peptide. This region also has lower turbidity than the initial because in order to be have colloidal stability all the nanocluster cannot be contained in the solution. This leave some nanocluster out of colloidal stability, which will directly affect the turbidity of the solution. This region is denoted by the green dashed line and the green test tube. The last region observable on these plots is the region of a large size but low turbidity. This region is denoted by the purple dashed lines and the purple test tube. The large size of the particles is due to the increase in peptide concentration. This high concentration coordinates more of the particles together into a very large size. Additionally his large size creates larger nanoclusters that disturbs colloidal stability and are pulled by gravity out of solution. This then causes a decrease in turbidity because the particles are too large to be disperse in solution.

Overall, together both the size vs. concentration and turbidity vs. concentration data proved a binding theory of how these particles interact and are coordinated with the designed peptide.

Chapter 4 : Conclusion

Overall, this thesis proved that a peptide sequenced to coat and coordinate IO particles could be successfully synthesized. It also showed that IO particles could be coordinated to larger sizes using a peptide. The particles fit within the 50 to 200nm size range that can takes advantage of the EPR effect. However, the sections that proved problematic were the synthesis and producing particles that were single sized particles rather than a nanocluster. For future works, the topics that would be explored further would be the synthesis of the particles. These particles were provide by the Hayes lab and the synthesis of could have contributed the dispersity of the particles. This would be explored to see if a single sized particle could be obtained. Additionally, other peptide architecture could be explored to see how a change in peptide structure can affects the size vs. peptide concentration profile. Overall this thesis provided a proof of concept that IO particles have the capacity to be controlled to a size that can utilize the enhance

permeability and retention effect. This concept can be further explored to create a contrast agent that can passive target cell and increase the odds in the fight against cancer.

BIBLIOGRAPHY

[1]Medical Imaging Modalities.” MITA RSS, National Electrical Manufacturers Association, www.medicalimaging.org/about-mita/medical-imaging-primer/.

[2]Berger, Abi. “Magnetic Resonance Imaging.” *BMJ : British Medical Journal* 324.7328 (2002): 35. Print.

[3]Automated Microwave Peptide Synthesizer.” *Liberty Blue - Automated Microwave Peptide Synthesizer*, cem.com/liberty-blue/.

[4]You, Fei, et al. "Biopanning and characterization of peptides with Fe 3 O 4 nanoparticles-binding capability via phage display random peptide library technique." *Colloids and Surfaces B: Biointerfaces* 141 (2016): 537-545

[5]Kobayashi, Hisataka, Rira Watanabe, and Peter L. Choyke. “Improving Conventional Enhanced Permeability and Retention (EPR) Effects; What Is the Appropriate Target?” *Theranostics* 4.1 (2014): 81–89. *PMC*. Web. 2 Nov. 2017.

[6]Allen TM, Cullis PR. Drug delivery systems: entering the mainstream. Science. 2004; 303:1818–22.

[7]Maeda H. The link between infection and cancer: Tumor vasculature, free radicals, and drug delivery to tumors via the EPR effect. Cancer Sci. 2013; 104:779–89

[8]Cyran CC, Sennino B, Fu Y, Rogut V, Shames DM, Chaopathomkul B. et al. Permeability to macromolecular contrast media quantified by dynamic MRI correlates with tumor tissue assays of vascular endothelial growth factor (VEGF) Eur J Radiol. 2012; 81:891–6

[9]Maeda H. Vascular permeability in cancer and infection as related to macromolecular drug delivery, with emphasis on the EPR effect for tumor-selective drug targeting. Proc Jpn Acad Ser B Phys Biol Sci. 2012; 88:53–71.

[10]Maeda H. The enhanced permeability and retention (EPR) effect in tumor vasculature: the key role of tumor-selective macromolecular drug targeting. Adv Enzyme Regul. 2001; 41:189–207.

[11]Maeda H, Nakamura H, Fang J. The EPR effect for macromolecular drug delivery to solid tumors: Improvement of tumor uptake, lowering of systemic toxicity, and distinct tumor imaging in vivo. Adv Drug Deliv Rev. 2013; 65:71–9.

[12]Kizaka-Kondoh S, Inoue M, Harada H, Hiraoka M. Tumor hypoxia: a target for selective cancer therapy. Cancer Sci. 2003; 94:1021–8

[13]Wang, Yi-Xiang J. "Superparamagnetic Iron Oxide Based MRI Contrast Agents: Current Status of Clinical Application." *Quantitative Imaging in Medicine and Surgery* 1.1 (2011): 35–40. *PMC*. Web. 2 Nov. 2017.

[14] Tanimoto A, Kuribayashi S. Application of superparamagnetic iron oxide to imaging of hepatocellular carcinoma. Eur J Radiol. 2006; 58:200–16.

[15] Wang YX, Hussain SM, Krestin GP. Superparamagnetic iron oxide contrast agents: physicochemical characteristics and applications in MR imaging. Eur Radiol. 2001; 11:2319–31.

ACADEMIC VITA

Academic Vita of Samuel Ajamu
SOA5395@PSU.EDU

Education

Major: Biomedical Engineering
Honors: Biomedical Engineering

Thesis Title: Peptide Coordinated Iron Oxide Nanoparticles for enhance MRI
Thesis Supervisor: Dr. Scott Medina

Work Experience

January 2018 – Present
Teaching Assistant, Tutor, University Park, PA
Pennsylvania State University Learning Center

- Predominately worked online with students using blackboard collaborate and communicated with instructors and students to facilitate content comprehension

July 2015- August 2016
Summer Sports Coach, Emmaus, PA
Push the Rock,

- Worked with children, specifically focusing on honing their skills in a variety of sports as well as educating them on the Christian morality and lifestyle.
- Orchestrated discussions in a large group of children, helping them to open up and work efficiently as a team.

Mehta Prep Academy August 2016
Tutor, State College, PA

- Worked with a small group of students on a student ran startup tutoring company.
- Focused mostly on sequestering clients and tutoring specifically.
- Gave me experience with taking initiative and business.

Awards: Pennsylvania State University LV Tutor of the Year 2016

Pennsylvania State University LV Public Speaking Competition 2016

Professional Memberships: Tau Beta Pi National Engineering Honors Society

Community Service Involvement: Community Service Chair (TAU BETA PI)
Remote Area Medical
Navigators Christian Organization Volunteering
Push the Rock Morocco Missions Trip

Language Proficiency: Yoruba